Spatial-Temporal Pattern of Land Use and SDG15 Assessment in the Bohai Rim Region Based on GEE and RF Algorithms

Lina Ke, Daqi Liu, Qin Tan, Shuting Wang, Quanming Wang, and Jun Yang

***Abstract*—The United Nations has proposed Sustainable Development Goal 15 (SDG15), which emphasizes the importance of sustainable land development. This study aims to use remote sensing data to build a spectral index feature dataset based on Google Earth Engine (GEE) platform, dig deep spectral features of ground objects, and use a random forest (RF) algorithm to extract land use type distribution data in the Bohai Rim region from 2000 to 2020. Meanwhile, combined with a land use transfer map and landscape pattern index, the spatio-temporal pattern of land use was quantitatively analyzed. Finally, the sustainable development level of land was evaluated quantitatively from three aspects: forest resource sustainability, wetland resource sustainability, and land system sustainability. The results show that the overall accuracy and kappa coefficient of land use classification achieved by GEE and the RF algorithm were 0.94 and 0.92, respectively. From 2000 to 2020, the main land use type in the study area was cropland, accounting for 33% of the total, and the impervious has significantly expanded, increasing by 9588.01 km^2, mainly from cropland, barren, and water. In relation to SDG15, forest resources exhibited poor stability, wetland resources demonstrated a steady recovery, SDG15.3.1 revealed that the problems of land degradation exist in various provinces and cities around the Bohai Sea, and the stability of the land system was poor between 2000 and 2020. This article can provide a valuable reference for land use management and ecological remediation in the Bohai Rim region.**

***Index Terms*—Bohai rim region, Google Earth Engine (GEE), land sustainability assessment, random forest (RF) algorithm, sustainable development goal 15 (SDG15).**

I. Introduction

LAND use/cover (LU/LC) effectively mirrors a region's economic vitality, capturing the impact of land intensity, policy orientation, and economic inputs within a distinct spatial-temporal context.

Since the 20th century, global urbanization has escalated, propelling land use and development to unprecedented levels [1], [2]. In this milieu, China's significant shifts in land spatial planning and use control have precipitated issues such as the overuse of prime arable land and ecological spaces, leading to ecological degradation and environmental pollution [3], [4]. As a pivotal coastal open development region in China, monitoring the Bohai Rim's LU/LC status is crucial for enhancing land use efficiency, evaluating sustainability, fostering coordinated regional development, and optimizing the region's overall benefits.

High-precision LU/LC mapping remains a central topic in land use change research [5]. Early studies were constrained by limited data, low precision, and small-scale analysis. However, advancements in data collection have enriched our understanding of multisource data, enabling long-term monitoring and enhanced time series analysis [6]. Remote sensing satellite imagery has become invaluable for accurate land use mapping. Google Earth Engine (GEE), as a comprehensive geographic data processing platform, allows access to extensive remote sensing datasets, facilitating analysis and processing through various programming languages, including JavaScript and Python [7], [8], [9], [10], [11]. Utilizing GEE, combined with advanced remote sensing image interpretation algorithms, has emerged as a leading approach in land use research. This method surpasses traditional automatic classification techniques, such as image element-based [12] and object-oriented classification [13], [14], and has progressed to more potent machine learning methods [15]. These techniques encompass convolutional neural networks, support vector machines (SVMs), decision trees, and random forests (RFs). Wu et al. [16] proposed a multilabel convolutional neural network model that exhibits superior performance in simulating complex mixed land use evolution compared to previous artificial neural network-cellular automata models. Yousefi et al. [17] optimized the SVM algorithm's parameters for LU/LC mapping, finding that a penalty parameter of >100 yielded more accurate results. The RF algorithm, integrating decision trees, has shown significant improvements in training speed and learning outcomes. Numerous studies have confirmed its efficacy in processing multisource data and various applications [18], [19], [20], [21]. Parthasarathy and Chandra compared the efficiency of three machine learning algorithms—RF, CART, and SVM—on the GEE platform for land use classification.

Manuscript received 24 December 2023; revised 6 March 2024; accepted 19 March 2024. Date of publication 22 March 2024; date of current version 5 April 2024. This work was supported in part by the Natural Science Foundation of Liaoning Province, China under Grant 2021-MS-274, in part by the National Natural Science Foundation under Grant 42076222, Grant 42276231, and Grant 42201070, and in part by the Social Science Federation Project of Liaoning Province, China under Grant 2024lslybkt-038. *(Corresponding author: Jun Yang.)*

Lina Ke, Daqi Liu, and Qin Tan are with the School of Geography, Liaoning Normal University, Dalian 116029, China (e-mail: linake@lnnu.edu.cn; bigqidq@foxmail.com; 13347672480@163.com).

Shuting Wang is with the Liaoning Earthquake Agency, Shenyang 110031, China (e-mail: wangshuting2017@163.com).

Quanming Wang is with the National Marine Environmental Monitoring Center, Dalian 116023, China (e-mail: qmwang@nmemc.org.cn).

Jun Yang is with the Jangho Architecture College, Northeastern University, Shenyang 110169, China, and also with the Human Settlements Research Center, Liaoning Normal University, Dalian 116029, China (e-mail: yangjun8@mail.neu.edu.cn).

Digital Object Identifier 10.1109/JSTARS.2024.3380580

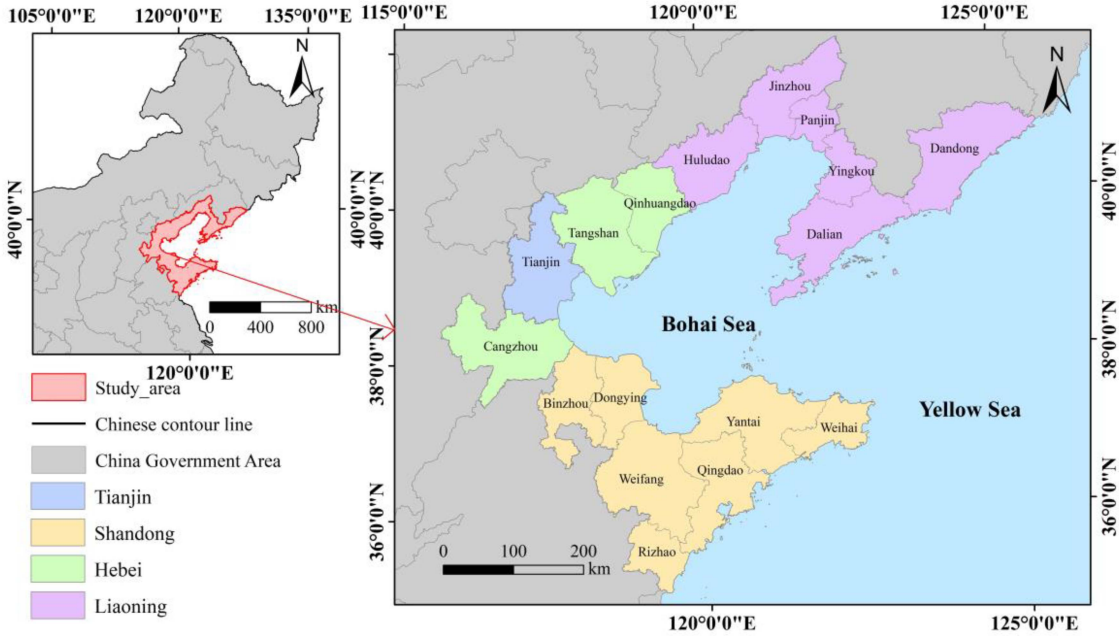

Fig. 1. Location map of the study area.

Their findings indicate that RF holds a considerable advantage in land use classification, especially in large-scale and complex feature areas [22].

For the objectives of sustainable development, the United Nations has established a set of 17 sustainable development goals (SDGs) [23]. Among these, Sustainable Development Goal 15 (SDG15), referred to as "Life on Land," embodies the concept of conservation and is seen as a critical benchmark for sustainable land use by 2030 [24]. Scholars have engaged in quantitatively assessing SDGs, with data selection and modeling method selection presenting key challenges in the assessment process [25]. Current quantitative assessments of SDG15, both domestically and internationally, tend to focus on individual objectives [26] and infrequently employ techniques such as GIS and spatial statistics. Moreover, due to regional variations, assessment methods and models suitable for one area may not be applicable elsewhere. This highlights the urgent need for more comprehensive research on multiscale quantitative monitoring and assessment of SDG15.

Therefore, the primary aim of this study is to enhance the implementation of the United Nations' SDGs at a local level in China. While existing research in this area is mostly qualitative, this study aims to contribute a quantitative dimension. Specifically, it focuses on SDG15-oriented monitoring and assessment of land resources. To achieve this, the study involves classifying wetland types, and employing GEE in conjunction with RF algorithms to produce detailed land use type maps for the Bohai Rim region for the years 2000, 2010, and 2020. In addition, it examines the spatial and temporal evolution of these areas. The study's specific objectives are as follows.

1) It utilizes open-access Landsat multisensor satellite imagery to accurately map land use types within the GEE, establishing an efficient and replicable workflow.
2) It employs high-precision, triphase, long-term series land use type maps to uncover and elucidate current land use changes, development patterns, and consequent landscape ecological effects in the Bohai Rim region, adopting both static and dynamic approaches.
3) It achieves dynamic, spatially detailed, and quantitative monitoring and assessment of selected SDG15 subtargets, aiming to provide scientific references and insights for promoting sustainable and coordinated development of land resources and ecology in the Bohai Rim region.

II. Materials and Methods

A. Overview of the Study Area

The Bohai Rim is located in the northern part of China along the west coast of the Pacific Ocean, which comprises the Liaodong Peninsula, the Shandong Peninsula, and the North China Plain in a "C"-shaped region. The Bohai Rim lies within the temperate monsoon climate zone, characterized by distinct seasonal variations and favorable light and water-heat conditions during summer [27]. The region's topography mainly consists of hills and plains, boasting abundant land resources. Liaoning and Shandong provinces, in particular, hold extensive coastline resources and a significant total scale of sea resources [28]. This region is rich in wetland resources, with a mudflat area of over $68.04*104\ km^2$ [29], concentrated in the Yellow River Delta and Liaohe River Delta, which provide abundant material products and ecological services for the regional socio-economy.

The Bohai Rim serves as a crucial gateway for China's northern region and the Northeast Asian Economic Zone [30]. Since the reform and opening-up era, this region has developed rapidly, becoming China's third largest urban economic zone after the "Yangtze River Delta" and "Pearl River Delta" urban

TABLE I
STATISTICS ON THE NUMBER OF IMAGES USED

imaging time	Data name	sensor device	Number of images /scene	Source
2000(01.01–12.31)	Landsat 5	TM	527	GEE(USGS)
	Landsat 7	ETM+	540	
2010(01.01–12.31)	Landsat 5	TM	452	
	Landsat 7	ETM+	422	
2020(01.01–12.31)	Landsat 7	ETM+	478	
	Landsat 8	OLI, TIRS	567	

TABLE II
CLASSIFICATION TABLE OF LAND USE TYPES

Number	Land use type	Including feature type
0	Barren	Barren
1	Cropland	Dryland, paddy fields
2	Forest	Woodland, shrubland, dredged woodland, and other woodland
3	Grassland	Grassland
4	Water	Rivers, lakes, reservoirs
5	Impervious	Urban land, rural residential land, other construction land
6	Wetland	Mudflat, Marshland

economic zones [31]. By 2019, the Bohai Economic Rim accounted for 18.5% of the country's total population, 18.3% of the country's total GDP, 16.7% of the country's total imports, and 17.1% of the country's total exports. The regional urbanization rate reached 64.91%, 4.31 percentage points higher than the national average.

With the rapid development of urbanization and industrialization in the Bohai Rim, coastal development activities have become increasingly frequent, land use has undergone significant changes, and the ecological environment is under unprecedented pressure. Large-scale cofferdams, dams, and other irrational marine development and utilization activities have resulted in a large loss of coastal wetlands. These factors have led to a continuous decline in the ecosystem service function and sustainable utilization of the Bohai Sea, threatening the economic and social development of the Bohai Sea's surrounding areas [32]. Thus, conducting SDGs assessment based on the Bohai Sea Rim is essential for maintaining the regional ecological balance and realizing the sustainable development of society, economy, and environment. In this study, the Bohai Sea Rim was selected as the study area, and the study area including 17 city-level administrative units was delineated by combining the research needs and the actual situation of the study area, as shown in Fig. 1.

B. Research Data and Preprocessing

The remote sensing data utilized in this research comprises Landsat 5 TM, Landsat 7 ETM+, and Landsat 8 atmospherically corrected surface reflectance image data. These datasets are readily accessible online via the GEE platform. The selected Landsat imagery encompasses data for the entire years 2000, 2010, and 2020, covering the study area (see Table I). Notably, Landsat data include a "pixel_qa" band, instrumental in identifying clouds and cloud shadows. To mitigate cloud interference, a CFMask cloud mask was implemented in GEE, filtering out images with cloud cover exceeding 10% for subsequent analysis. Challenges in unprocessed image data often stem from cloud cover, cloud shadows, and anomalies in Landsat 7 ETM+ data [33].

The research area is situated in the Bohai Rim region. In accordance with the prevailing land use classification system and considering the subsequent land landscape utilization objectives, the Bohai Rim region has been categorized into seven distinct land types (including Wetland, Cropland, Forest, Grassland, Water, Impervious, and Barren) based on a comprehensive analysis of research goals as well as natural conditions such as topography, climate, and hydrology. Refer to Table II for detailed information.

For the selection of sample points, this study uses Google Earth images and visual interpretation. In order to ensure that the selected training samples conform to the principles of representativeness, uniformity, and quantity, this article evenly divides the research area into six equal "block" elements according to the maximum boundary for sample selection. This "block" based partitioning method can ensure that the selected samples are evenly distributed in the research area. Each region assigned 500 sample points for each land use type, for a total of 21 000 sample points. These points were incorporated into GEE, of which 70% were randomly selected for training the RF model and the remaining 30% were allocated for accuracy verification of the classification results.

III. RESEARCH METHODS

The main content of this study contains the following three aspects: 1) land use classification based on GEE; 2) characterization of land use change; and 3) sustainable development assessment based on SDG15. The technical route of the study is shown in Fig. 2.

A. Random Forest Model

RF algorithm belongs to ensemble learning, which has the advantages of high accuracy, low error, strong robustness, and strong antinoise ability [34]. In this study, a classification feature set consisting of Landsat remote sensing image original spectral bands and multiple spectral feature indices is constructed. The spectral feature index can expand the pixel difference of adjacent

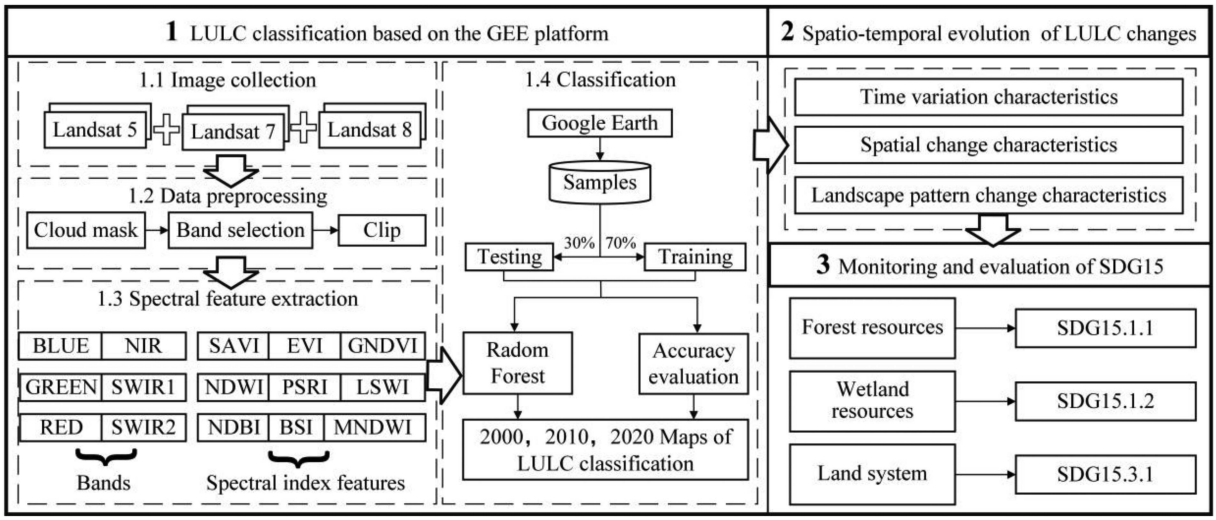

Fig. 2. Technology Roadmap.

TABLE III
DESCRIPTION OF THE FEATURES

classification feature	abbreviation	Calculation formula	Feature description
spectral feature	B	BLUE、GREEN、RED、NIR、SWIR 1、SWIR 2	Reflect different spectral reflection characteristics
vegetation index	NDVI	$(B_{NIR} - B_{RED})/(B_{NIR} + B_{RED})$	Reflect crop growth and nutrition information
	SAVI	$(\mathrm{B_{NIR}} - \mathrm{B_{RED}}) \times (1 + \mathrm{L}) /(\mathrm{B_{NIR}} + \mathrm{B_{RED}} + \mathrm{L})$	Soil-Adjusted Vegetation Index
	GNDVI	$(B_{NIR} - B_{GREEN})/(B_{NIR} + B_{GREEN})$	Green Normalized Difference Vegetation Index
	PSRI	$(B_{RED} - B_{BLUE})/B_{NIR}$	A vegetation index used to assess the degree of aging of vegetation
water index	NDWI	$(\mathrm{B_{GREEN}} - \mathrm{B_{NIR}})/(\mathrm{B_{GREEN}} - \mathrm{B_{NIR}})$	It is used to extract water information
	LSWI	$(\mathrm{B_{NIR}} - \mathrm{B_{SWIR1}})/(\mathrm{B_{NIR}} + \mathrm{B_{SWIR1}})$	Land Surface Water Index
	MNDWI	$(\mathrm{B_{GREEN}} - \mathrm{B_{SWIR1}})/(\mathrm{B_{GREEN}} + \mathrm{B_{SWIR1}})$	Modified Normalized Difference Water Index
Building index	NDBI	$(\mathrm{B_{SWIR1}} - \mathrm{B_{NIR}})/(\mathrm{B_{SWIR1}} + \mathrm{B_{NIR}})$	Reflecting the building land information, the larger the value, the higher the building density
soil index	BSI	$((\mathrm{B_{SWIR1}} + \mathrm{B_{RED}}) - (\mathrm{B_{NIR}} + \mathrm{B_{BLUE}})) /((\mathrm{B_{SWIR1}} + \mathrm{B_{RED}}) + (\mathrm{B_{NIR}} + \mathrm{B_{BLUE}}))$	Bare Soil Index, assess and monitor bare land area and changes

ground objects [9] and it has been proposed that the phenological difference of LULC type should be considered to improve the classification accuracy [35], [36], [37].

Therefore, this study took into account the uneven image distribution caused by the seasonal changes of surface features, especially vegetation features, and designed a spectral index feature dataset including Landsat's main original single-band features, vegetation index, water index, building index, and soil index according to the phenological characteristics of vegetation in the study area. The total number of features was 45 ($6 \times 3 + 9 \times 3 = 45$). Using the seasonal percentage feature can better reduce the classification errors caused by regional seasonal fluctuations and further improve the classification accuracy of the RF algorithm. A detailed description of each feature is given in Table III.

Invoking the RF classifier in GEE usually requires setting two parameters: the number of feature variables selected at each separation point (mtry) and the number of tree classifiers (Ntrees), which will affect the performance and complexity of the model. Increasing the number of Ntrees can improve the performance of the model, making it more robust and generalization ability. A proper mtry can make the model more robust and reduce the risk of overfitting. In this article, after parameter adjustment, the ntree parameter is set to 100 trees, and the square root of

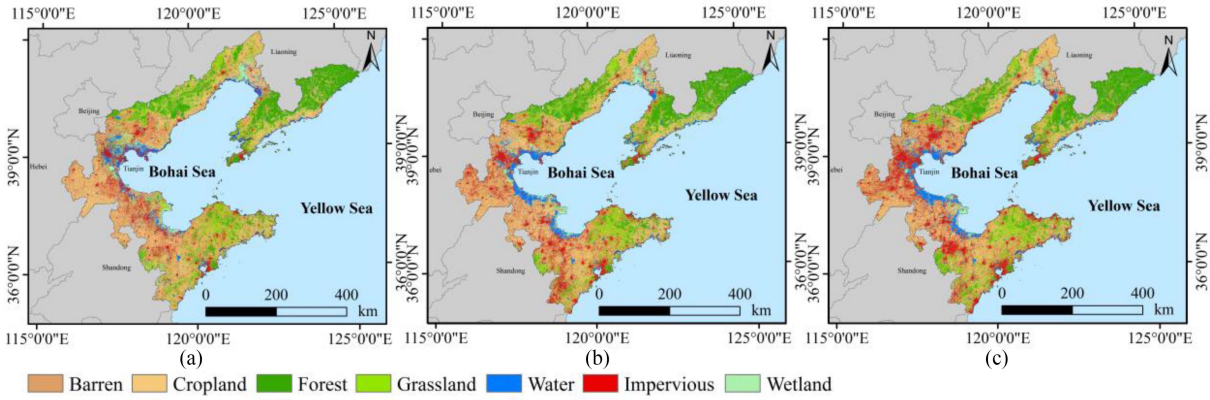

Fig. 3. (a) 2000, (b) 2010, and (c) 2020 land use classification map of the Bohai Rim region.

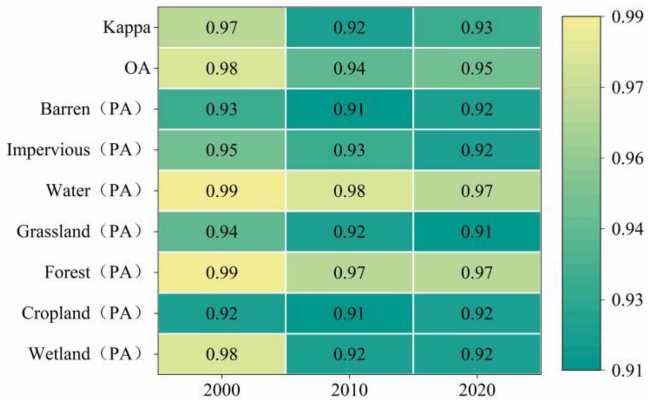

Fig. 4. Accuracy picture of land use classification results.

TABLE IV
COMPARISON WITH OTHER LAND USE DATASETS

Product		This article	Globe Land	World Cover
Barren	PA	0.92	0.59	0.32
Cropland	PA	0.92	0.66	0.78
Forest	PA	0.97	0.69	0.56
Grassland	PA	0.91	0.53	0.26
Water	PA	0.97	0.74	0.58
Impervious	PA	0.92	0.71	0.48
Wetland	PA	0.92	0.48	0.59
OA		0.95	0.63	0.44
Kappa		0.93	0.57	0.35

the number of features involved in mtry and classification is calculated.

B. Land Use Classification Results and Accuracy Evaluation

Based on the GEE platform, this section finally obtains the land use distribution results of the Bohai Rim in 2000, 2010, and 2020 by mining the classification feature set, followed by utilizing the RF algorithm with high classification accuracy, as shown in Fig. 3.

The verification scheme in this article is comprised of three primary components: response design, sampling design, and analysis. In the response design, the spatial evaluation unit is defined as a Landsat pixel measuring 30 m × 30 m. The reference classification for validation purposes is determined using high spatial resolution data obtained freely from Google Earth [38]. From Fig. 4, it can be found that the land use classification system based on RF classification in this article achieves better accuracy; the overall accuracy is between 0.94 and 0.98, and the Kappa coefficient is greater than 0.92. Overall, the results can meet the needs of the subsequent land use analysis and research, and the analysis results obtained are reliable.

The land use classification results of the Bohai Rim region in this article were compared with GlobeLand30 and World Cover v100 land use datasets, and the accuracy of the classification results was tested with 2020 as the sample. The former is derived from the National Catalogue Service for Geographic Information, The latter was obtained from the World Cover v100, a 10-m resolution land cover data product released by the European Aviation Agency ESA in 2020, with an overall accuracy of 74.4%. The classification system of the two datasets was reclassified to make it consistent with the classification system of this study. The sample point data generated in this article was used to sample the products of the dataset, generate a confusion matrix, and evaluate the accuracy of classification results with existing open land use datasets. As given in Table IV, the classification map of the Bohai Rim region completed by spectral characteristics and RF classification method in this article achieved the best classification accuracy, the overall accuracy was 0.95, and the Kappa coefficient was 0.93, which was significantly higher than other global scale land use products. From the perspective of producer accuracy (PA), the classification results of this article also have overall advantages. For wetland land classes with greater difficulty in classification, this study can still achieve a higher classification accuracy (0.92), which reflects better accuracy of the classification results in this study compared with 0.63 in GlobeLand and 0.59 in WorldCover.

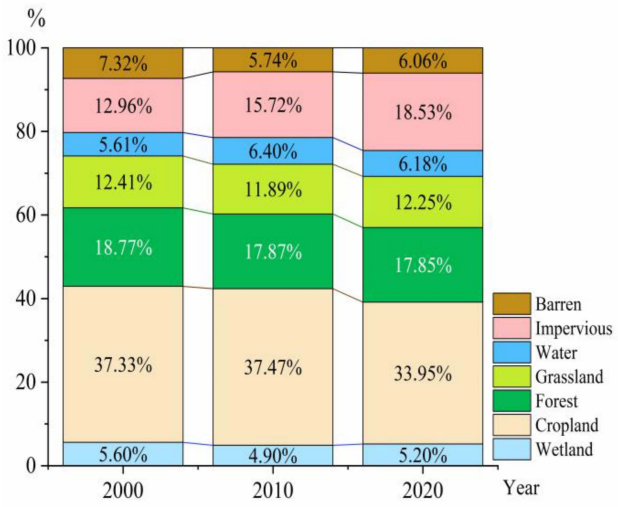

Fig. 5. Proportion of land use types in the Bohai Rim region from 2000 to 2020.

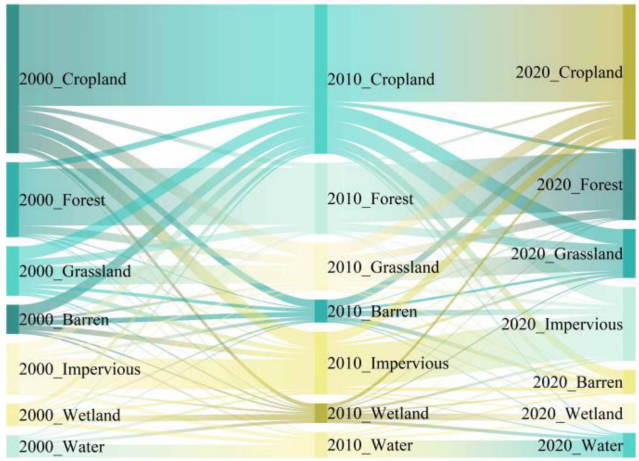

Fig. 6. Sankey map of the transfer land use types in the study area from 2000 to 2020.

IV. Result Analysis

A. Analysis of Spatial and Temporal Evolution of Land Use

The dominant land use type in the Bohai Rim from 2000 to 2020 was arable land (see Fig. 5), and between 2000 and 2020, impervious expanded rapidly, increasing by 9588.01 km^2; the area of water bodies also showed a small increase of about 980.53 km^2; the area of all other types of land showed a different level of decrease. The primary factor contributing to the decline in the area of these land types was the continuous expansion of impervious.

1) Characterization of Temporal Changes in Land Use: The land use transfer matrix delineates the transitions among different land types within the study area over the specified period [39]. It provides detailed insights into the dynamic interactions and exchanges between various land use types. Using ArcGIS 10.6, the dynamic land use transfer matrices for 2000–2010 and 2010–2020 were constructed and subsequently visualized in a Sankey diagram (see Fig. 6).

During 2000–2010, significant transfers out were observed from unutilized land, forest, wetlands, and cropland. The primary recipients of these land transfers were cropland and impervious. Similarly, in the 2010–2020 period, cropland exhibited the largest area of transfers out of all land types, with the pattern of transfers mirroring the previous decade.

Overall, from 2000 to 2020, the Bohai Rim region experienced a substantial expansion of impervious, predominantly sourced from arable land, barren, and water bodies. The transformed areas for these were 9218.30 km^2, 2889.99 km^2, and 1607.74 km^2, respectively. This trend highlights the rapid urbanization in the Bohai Rim, characterized by the overconsumption of soil and water resources.

2) Spatial Change Characteristics of Land Use: A land use transfer graph, an analytical method that combines temporal and spatial elements, was employed in this study to construct a land use transfer map of the Bohai Rim region for 2000–2020. Based on the theory of land use transfer graph, a total of 49 types of graph units were generated, with 42 types experiencing changes in land use. According to the transferred area data (see Table V) and the spatial distribution illustrated in the land use transfer atlas (see Fig. 7), it was observed that 12 types of atlas units accounted for a cumulative change rate of 63.02%. These units exhibited significant geographical disparities across the Bohai Rim region. The most extensive transfer was observed from "cropland to impervious" (code 15), predominantly occurring in Weifang, Rizhao, and Binzhou cities in Shandong Province, Cangzhou City, Tangshan City, and southern Qinhuangdao in Hebei Province, along with coastal areas of other cities. Notably, this conversion was most pronounced in the city centers of Weifang, Cangzhou, and Tangshan. The second-largest transfer was "cropland to grassland" (code 13), occurring across all areas of the three provinces and one city in the Bohai Rim, attributed to China's ecological initiative of converting farmland back to forest and grassland. The third significant transfer was "grassland to cropland" (code 31), primarily found in Yantai, Qingdao, Weifang, Rizhao, and Dongying in Shandong Province and Jinzhou and Huludao in Liaoning Province.

3) Analysis of Land Use Landscape Pattern Changes: As a key indicator of the impact of urbanization on the regional ecological environment, landscape pattern evolution analysis has been widely used in the study of land use patterns. In this study [40], 90 m resolution was chosen as the optimal granularity for landscape analysis. Ten landscape pattern indices were used to evaluate the structural characteristics of land use landscape pattern change. The Fragstats 4.2 software was used for analysis, and the changes of these indicators were comprehensively analyzed in the three dimensions of patch level, patch type level, and landscape level in Table VI and Fig. 8, and the main conclusions were drawn as follows.

The maximum patch index (LPI) in the study area decreased by 22.33%, and the cohesion index remained relatively stable, indicating that the area of dominant landscape species decreased during this period but the connectivity between landscape patches was still good, and the ecosystem in the study area

TABLE V
UNIT ORDINATION TABLE OF LAND USE TRANSFER GRAPH IN STUDY AREA FROM 2000 TO 2020

Encoding	Land use transfer map unit	Number of mapping units/unit	Transfer area/km^2	Change ratio/%
15	Cropland→Impervious	10 242 559	9218.30	11.28%
13	Cropland→Grassland	7 516 735	6765.06	8.28%
31	Grassland→Cropland	6 354 593	5719.13	7.00%
01	Barren→Cropland	5 271 859	4744.67	5.81%
23	Forest→Grassland	4 447 836	4003.05	4.90%
10	Cropland→Barren	4 202 264	3782.04	4.63%
51	Impervious→Cropland	4 176 023	3758.42	4.60%
32	Grassland→Forest	3 739 256	3365.33	4.12%
05	Barren→Impervious	3 211 100	2889.99	3.54%
35	Grassland→Impervious	2 786 538	2507.88	3.07%
12	Cropland→Forest	2 691 158	2422.04	2.96%
16	Cropland→Wetland	2 579 507	2321.56	2.84%
	aggregate	57 219 428	51497.49	63.02%

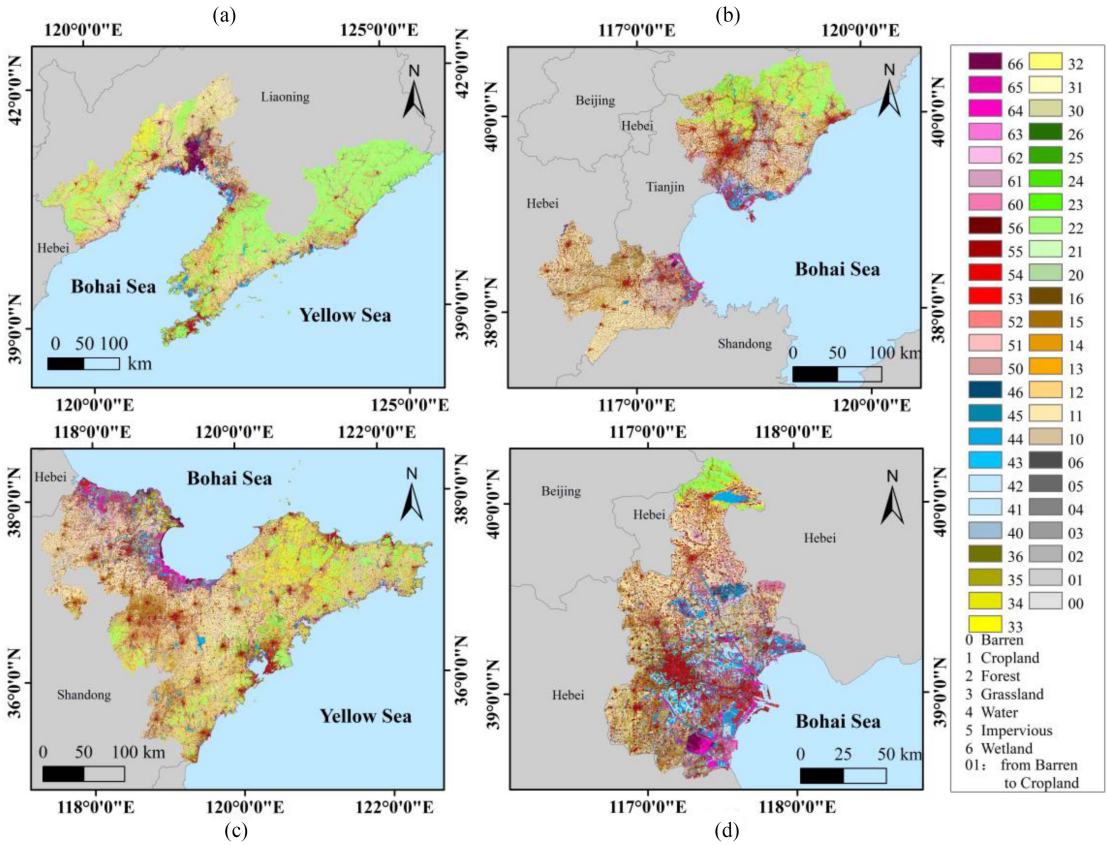

Fig. 7. Map of land use transfer in the Bohai Rim region from 2000 to 2020. (a) Research area of Liaoning Province. (b) Research area of Hebei Province. (c) Research area of Shandong Province. (d) Tianjin City.

had a certain degree of integrity. However, increased human disturbance has led to fragmentation of the landscape. The number of patches (NP) showed a fluctuating upward trend, increasing by 9.93%. Edge density (ED) decreased first and then increased significantly, with an overall increase of 4.17%.

This change may reflect the instability of the landscape boundary in the Bohai Rim region and further reflect the complexity of the ecosystem. The Landscape Index (LSI) increased by 4.12% overall. This indicates that the landscape pattern around the Bohai Sea has evolved into a more complex and irregular form. This change may have a certain impact on the stability of the ecosystem and biodiversity. Notably, the interleaved Juxtaposition index (IJI) continued to decline by 3.38%. This trend is unfavorable to biodiversity and ecological functions,

TABLE VI
INDEX TABLE OF LANDSCAPE PATTERNS IN THE BOHAI RIM REGION FROM 2000 TO 2020

landscape pattern index	2000	2010	2020
Number of plaques (NP)	2 049 453	1 974 904	2 252 964
Area ratio of the largest plaque (LPI)	7.21	4.38	5.60
Average plaque size (MPS)	8.40	8.72	7.64
ED	78.93	75.68	82.22
Shape index (LSI)	827.20	793.49	861.29
Dispersion and juxtaposition index (IJI)	88.07	85.39	85.09
Binding index (COHESION)	99.26	99.31	99.17
Spread index (CONTAG)	25.91	27.78	25.46
SHDI	1.72	1.71	1.74
SHEI	0.884	0.878	0.894

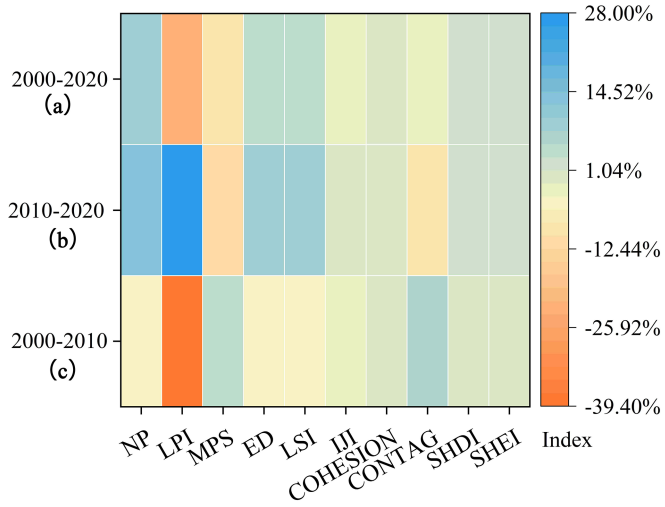

Fig. 8. Landscape pattern index growth map from 2000 to 2020. (a) 2000–2010. (b) 2010–2020. (c) 2000–2020.

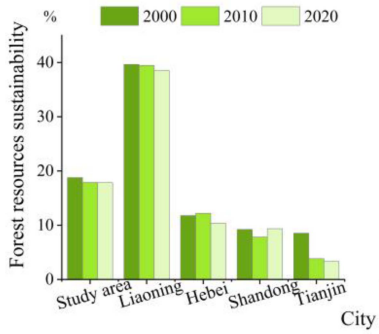

Fig. 9. Forest resource sustainability of the Bohai Rim region and provinces from 2000 to 2020.

and attention should be paid to ecological protection in the Bohai Rim region. The turning point in the Shannon diversity index (SHDI) from decline to increase occurred in 2010–2020, from 1.72 to 1.74, an overall increase of 1.16%. This reflects the diversification of landscape types, the increasing degree of fragmentation, and the impact on ecological functions in the Bohai Rim region in the past 20 years.

To sum up, the changes in landscape patterns in the Bohai Rim region in the last 20 years have presented complex and diverse characteristics. In the future ecological protection and restoration work, we should fully consider these changes and formulate targeted policies and measures to achieve sustainable development of the ecosystem. At the same time, the monitoring and evaluation work will be strengthened to provide a scientific basis for ecological protection and ecological civilization construction in the Bohai Rim region.

B. SDG15 Sustainability Analysis

The core objectives of SDG15 are to protect, restore, and promote the sustainable use of terrestrial ecosystems, sustainably manage forests, combat desertification, halt and reverse land degradation, and halt biodiversity loss, and the SDG15 indicator framework contains 12 targets and 14 indicators. At present, the design of the indicator framework and the calculation method of the indicator are still worthy of discussion. In summary, considering the accessibility and operability of the indicator data and the resource endowment of the Bohai Rim region, the research focuses on evaluating the progress of SDG15.1 and SDG15.3 targets.

1) Forest Resource Sustainability: SDG15.1 emphasizes the protection, restoration, and sustainable use by 2020 of terrestrial and inland freshwater ecosystems and their services, in particular, forests, wetlands, foothills, and drylands, in accordance with obligations under international agreements. In this study, the recommended index SDG15.1.1 was used to represent the sustainability of forest resources as the proportion of forest area to the total area of LULC (except inland water bodies) (see Fig. 9). The target value of SDG15.1.1 in the Bohai Rim region during 2000–2020 has decreased from 18.77% in 2000 to 17.85% in 2020. It shows that forest resources are scarce and forest degradation exists in the Bohai Rim region. Among them, rapid economic development and population increase are the main reasons. In addition, the different natural resource endowments, regional blockades, and different development levels in

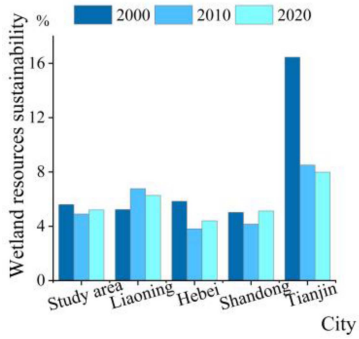

Fig. 10. Wetland resources sustainability of the Bohai Rim region and provinces from 2000 to 2020.

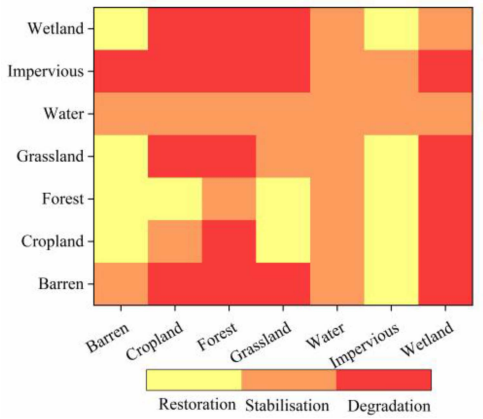

Fig. 11. Definition of land degradation.

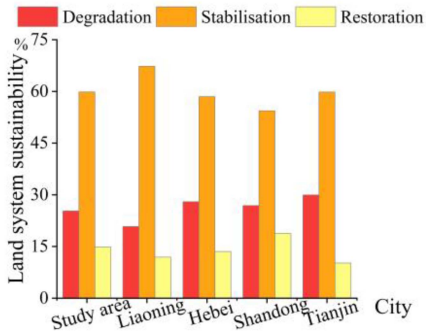

Fig. 12. Land system sustainability of the Bohai Rim region and provinces from 2000 to 2020.

the Bohai Rim region lead to the uneven distribution of forest resources among provinces and cities, and the variation trend among regions is quite different.

2) Wetland Resources Sustainability: As one of the key open development areas in China, the Bohai Rim region has a more serious degree of wetland fragmentation, which deserves separate attention. Therefore, the sustainability of wetland resources is taken as an indicator factor in the assessment of SDG15.1.2, which covers the connotation of protecting wetlands as a terrestrial ecosystem. In this study, the proportion of wetland area to the total land area was used to characterize the sustainability of wetland resources (see Fig. 10). During 2000–2020, the wetland resources in the Bohai Rim region first decreased and then increased but still showed a decreasing trend in general, from 5.60% in 2000 to 5.20% in 2020, reflecting the trend of wetland degradation first and then slow recovery during the study period. The reason is that there are many wetland resources around the Bohai Sea. However, since the 1980s, excessive wetland reclamation in the Bohai Rim region has resulted in a sharp reduction in the area of natural coastal wetlands [40], and the problem of wetland degradation has become increasingly prominent. Since 2018, The State Council has requested that ecological restoration projects be actively promoted to gradually restore damaged wetlands.

3) Land System Sustainability: SDG15.3 aims to achieve the protection, restoration, and sustainable utilization of terrestrial ecosystems and their biodiversity by 2030 while also preventing land degradation. To assess the extent of land degradation in the Bohai Rim region, this article adopts land cover change as an indicator based on the good practice guidance on SDG 15.3 issued by the United Nations Convention to Combat Desertification. The definition of land degradation used in this study is consistent with previous relevant research findings (see Fig. 11).

To examine land system sustainability in the Bohai Sea Rim, SDG15.3.1 was calculated, and the spatial distribution of land degradation was mapped (see Figs. 12 and 13). Fig. 12 reveals that from 2000 to 2020, the Bohai Sea Rim faced significant land degradation, indicating poor land system sustainability. Notably, Tianjin experienced the most extensive land degradation, indicating poor land system sustainability. As depicted in Fig. 13(a)–(d), the spatial distribution of degraded land varies. Land in the central areas of each province is relatively stable, primarily due to its use as impervious, which has seen minimal change over the study period. Conversely, the peripheral areas, largely comprised of cropland, exhibit a wider distribution of degradation.

V. Discussion

A. Comparison With Different Algorithms

Traditional classification methods (visual interpretation) are difficult to avoid the impact of "different spectrum of the same object" and "foreign body of the same spectrum" in land use classification, and there are many misclassifications and missing classification problems [41], while many studies have found that machine learning algorithms, such as SVMs, decision trees, and RFs, can achieve good classification results [42], [43].

The principle of the artificial neural network is to construct a subspace with a complex classification interface based on the nonlinear system space and simulate the human learning process to determine the relationship between the input layer and the output layer. However, the classification accuracy of this method is subject to the feature parameters and classifier parameters in the process of application [44]. As a supervised classification method, SVM has significant advantages in the classification of land use in small areas [45]. Different from the artificial neural network, the decision tree method is essentially data mining, which is more suitable for processing multidimensional data

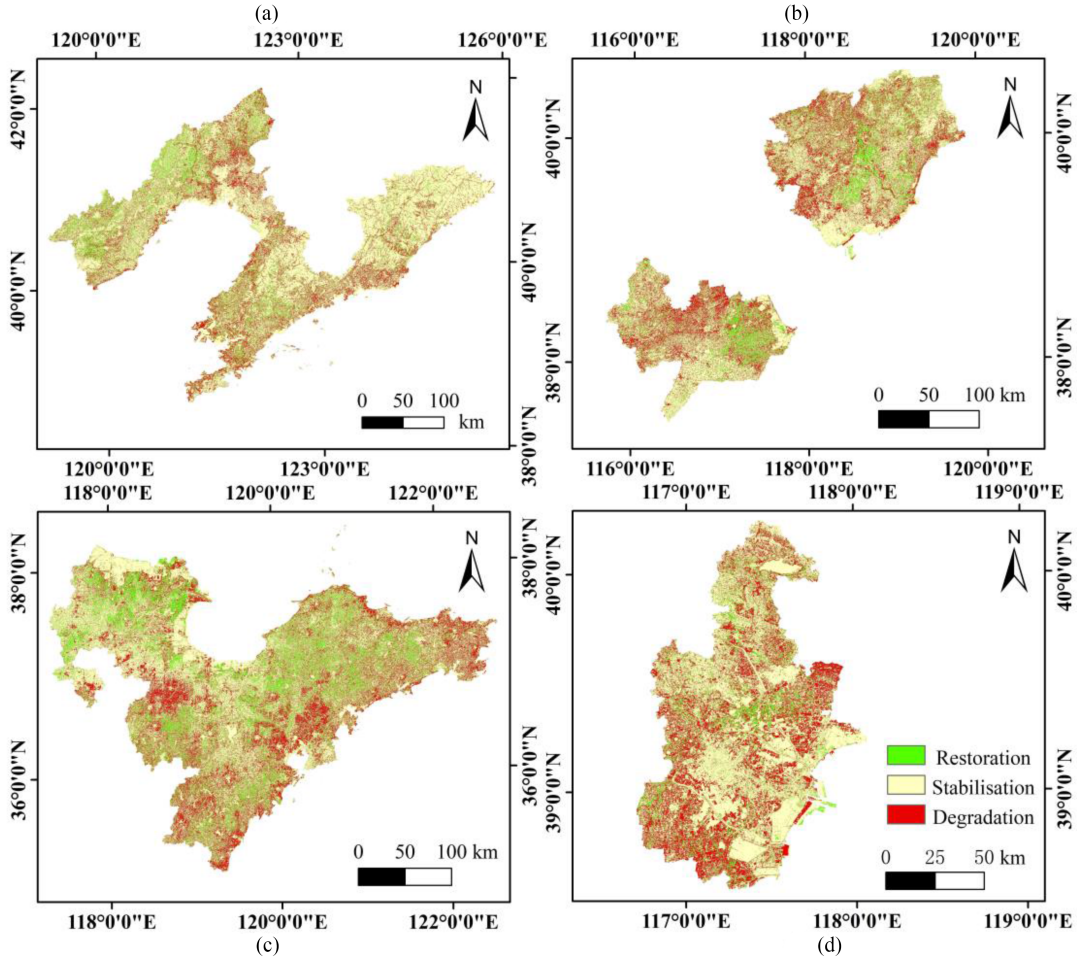

Fig. 13. Land degradation distribution map of Bohai Rim region from 2000 to 2020. (a) Research area of Liaoning Province. (b) Research area of Hebei Province. (c) Research area of Shandong Province. (d) Tianjin City.

[46]. RF algorithm integrates decision tree, and training speed and learning effect are significantly improved, and it has the advantages of high accuracy, small error, strong robustness, and strong antinoise ability. At the same time, the RF algorithm has excellent application effect in processing multisource data and other fields [47]. Parthasarathy and Chandra [22] compared the efficiency of three machine algorithms, RF, CART, and SVM, in LULC classification on the GEE platform, and the results proved that RF had significant advantages in LULC classification and was more suitable for land type classification research in a large range and complex terrain areas. Therefore, GEE combined with the RF algorithm was selected for land use classification in this study.

B. *Extraction of Land Use Types*

Accurate extraction of land use types is pivotal in this study. The Bohai Rim area, characterized by its vast expanse, is classified using intra-annual, long-duration, dense sequence imagery, and time-series feature sets based on phenology. Managing and processing this substantial geospatial dataset poses a challenge in achieving high-performance computation. GEE, a cloud-based platform, offers free access to robust computational resources for processing diverse geospatial datasets [48]. In this research, GEE's cloud computing capabilities, along with its integrated machine learning and image processing algorithms, were employed to accurately extract three annual land use types in the study area. GEE facilitates the development of remote sensing imagery information extraction methods with higher automation, reducing the time required for data acquisition, calibration, and preprocessing. However, limitations exist, such as constraints on the number of points in the training set for machine learning algorithms, which can be addressed by processing data in segments.

Improvements can still be made to the land use classification process. First, higher resolution satellite images or multisource remote sensing data fusion could be considered for better data selection. Second, in feature set selection, aspects such as topography and texture have not been included. Enhancing the feature set and selecting highly relevant feature variables for training could further optimize accuracy. Future studies might explore GEE's segmentation algorithms to enhance object-based classification methods. The efficacy of combining multiple machine

learning algorithms, as opposed to solely using the RF classifier, in improving classification accuracy remains to be tested.

Furthermore, since wetland types are separately categorized in this study, defining wetlands accurately is essential [49]. The focus on coastal wetlands necessitates further consideration of coastline extraction. Remote sensing data sensitive to moisture, such as SAR images, could be utilized, and wetland-related indices might be added to the feature set to refine the classification process.

C. Spatial and Temporal Evolution of the Bohai Sea Region

This study analyzes the spatial and temporal evolution of land use in the Bohai Sea region over the past 30 years, employing land use transfer matrices and mapping. The findings reveal significant encroachment and destruction of arable land during the study period, leading to the compensatory occupation of natural ecological lands such as grasslands and wetlands. This widespread conversion, affecting various land types including cropland, impervious, grassland, and wetland, highlights the lack of strategic planning in the utilization of land resources in the Bohai Rim. Such practices have resulted in low resource efficiency and wastage. To gain deeper insights, this driving mechanism should further be quantitatively analyzed in conjunction with habitat quality changes [50] and ecosystem service values [51], providing scientific guidance for ecological environment construction in the Bohai Rim.

The landscape pattern index, which is a quantitative indicator that captures both landscape structure and spatial features, holds significant ecological importance. Analyzing this index across three dimensions—patch level, patch type level, and landscape level—indicates that increasing landscape fragmentation has progressively impaired the ecosystem structure and functions in the Bohai Rim region, causing severe damage to the value of ecological services. Future research should focus on identifying and analyzing the key factors influencing landscape patterns, including urbanization, policy, mining, population growth, and natural factors such as climate and soil. These factors are vital in driving landscape change, and their in-depth study is crucial for understanding and mitigating their impact on the region's ecology.

D. Assessment of SDG15 Objectives

Current research urgently needs to enhance quantitative monitoring and assessment of SDG15 subtargets. In this study, land use type maps for 2000, 2010, and 2020 serve as the baseline for spatio-temporal analysis, aligning with specific SDG15 subtargets. The sustainability of forest resources corresponds to the SDG15.1.1 target, wetland resource sustainability corresponds to the SDG15.1.2 target, and land system sustainability corresponds to the SDG15.3.1 target. For SDG15.1.1, the focus is on the protection and restoration of wetlands and other habitats. This study evaluates wetland resource sustainability using the proportion of wetlands in the total land area, with future research planning to incorporate additional factors, such as wetland morphology, habitat quality, and productivity.

In assessing land system sustainability in the Bohai Sea region, the SDG15.3.1 target was employed, defined as "the proportion of degraded land to the total land area." The evaluation of degraded land should include subindicators such as changes in land use types, land productivity, and carbon stocks both above and below ground. Due to data availability constraints, this study simplifies SDG15.3.1 by focusing solely on land use change data and the definition of degraded land types, thus limiting the scope of the assessment.

In conclusion, while this research addresses three key subtargets of SDG15, it is imperative to expand the scope to include additional targets, such as SDG15.8, and to analyze the interplay among these subtargets. Moreover, the assessment of SDG15 in this article relies on a single dataset. Future studies should integrate a broader array of data—including population, land use, net primary productivity, soil organic carbon, the distribution of flora and fauna, nature reserve boundaries, and key biodiversity areas—to enrich the assessment's comprehensiveness and accuracy.

VI. Conclusion

In this article, with the help of massive remote sensing data provided by the GEE platform and powerful cloud computing capability, the spectral characteristics of ground objects are deeply mined, and the RF algorithm is used to extract the LULC-type distribution data of three periods from 2000 to 2020 in the Bohai Rim region. Based on the LULC-type area, land use transfer matrix, land use transfer map, and landscape pattern index, the LULC change pattern in the study area in the past 20 years was analyzed from multiple perspectives. Finally, according to the sustainable development goals of SDG15, the sustainable development of land resources in the Bohai Rim region is quantitatively analyzed. This study provides countermeasures and suggestions for structural optimization and layout regulation of land use transition to sustainable development, alleviates the increasingly sharp contradiction between people and land in the Bohai Rim region, and actively implements the development strategy of ecological civilization construction in China.

The results show that the GEE cloud platform combined with the RF algorithm can achieve reliable LULC classification results. From 2000 to 2020, the impervious in the Bohai Rim region has always maintained an expanding trend. Human activities have led to the decrease of landscape-dominant species, the diversification of landscape types, the intensification of landscape fragmentation, and the damage of ecological functions. According to SDG15.1.1, the sustainability of the overall forest resources in the Bohai Rim region decreased during 2000–2020. Corresponding to SDG15.1.2, the sustainability of wetland resources fluctuated, decreased first and then increased, but still decreased in general. According to SDG15.3.1, all provinces and cities around the Bohai Sea have different degrees of land degradation, and the sustainability of the land system is poor.

References

[1] G. He, K. Wang, Q. Zhong, G. Zhang, C. K. van den Bosch, and J. Wang, "Agroforestry reclamations decreased the CO2 budget of a coastal wetland in the Yangtze estuary," *Agricultural Forest Meteorol.*, vol. 296, 2021, Art. no. 108212.

[2] E. Esa, M. Assen, and A. Legass, "Implications of land use/cover dynamics on soil erosion potential of agricultural watershed, northwestern highlands of Ethiopia," *Environ. Syst. Res.*, vol. 7, pp. 1–14, 2018.

[3] Y. Wenze, W. Tianyu, and Z. Yanlin, "Unified zoning of territorial space use control derived from the core concept of three types of spatial zones and alert-lines," *China Land Sci.*, vol. 34, pp. 52–59, 2020.

[4] Y. Wenze, W. Tong, W. Tianyu, and X. Hao-xuan, "'Double evaluations' for territorial spatial planning: Challenges and responses," *J. Natural Resour.*, vol. 35, pp. 2299–2310, 2020.

[5] A. Vali, S. Comai, and M. Matteucci, "Deep learning for land use and land cover classification based on hyperspectral and multispectral earth observation data: A review," *Remote Sens.*, vol. 12, 2020, Art. no. 2495.

[6] B. Xue, H.-Q. Li, B.-J. Huang, and H. Wang, "Data-driven study of complex socio-economic-natural ecosystems: Scales, processes and decision linkages," *Chin. J. Appl. Ecol.*, vol. 33, no. 12, pp. 3169–3176, 2022.

[7] M. Amani et al., "Canadian wetland inventory using Google Earth Engine: The first map and preliminary results," *Remote Sens.*, vol. 11, 2019, Art. no. 842.

[8] H. Tamiminia, B. Salehi, M. Mahdianpari, L. Quackenbush, S. Adeli, and B. Brisco, "Google Earth Engine for geo-Big Data applications: A meta-analysis and systematic review," *ISPRS J. Photogrammetry Remote Sens.*, vol. 164, pp. 152–170, 2020.

[9] L. G. Santhosh and D. N. Shilpa, "Assessment of LULC change dynamics and its relationship with LST and spectral indices in a rural area of Bengaluru district, Karnataka India," *Remote Sens. Appl.*, vol. 29, 2023, Art. no. 100886.

[10] S. Aldiansyah and R. A. Saputra, "Comparison of machine learning algorithms for land use and land cover analysis using google earth engine (case study: Wanggu watershed)," *Int. J. Remote Sens. Earth Sci.*, vol. 19, 2023, Art. no. 197.

[11] Z. Zhao et al., "Comparison of three machine learning algorithms using Google Earth Engine for land use land cover classification," *Rangeland Ecol. Manage.*, vol. 92, pp. 129–137, 2024.

[12] R. Goldblatt et al., "Using Landsat and nighttime lights for supervised pixel-based image classification of urban land cover," *Remote Sens. Environ.*, vol. 205, pp. 253–275, 2018.

[13] F. Shi et al., "Assessing land cover and ecological quality changes in the forest-steppe ecotone of the Greater Khingan Mountains, Northeast China, from Landsat and MODIS observations from 2000 to 2018," *Remote Sens.*, vol. 14, 2022, Art. no. 725.

[14] A. A. Kozlova, A. V. Khyzhniak, I. A. Piestova, and A. A. Andreiev, "Synergetic use of Sentinel-1 and Sentinel-2 data for analysis of urban development and green spaces," in *Proc. 17th Int. Conf. Geoinform.- Theor. Appl. Aspects*, 2018, pp. 1–6.

[15] J. Wang, M. Bretz, M. A. A. Dewan, and M. A. Delavar, "Machine learning in modelling land-use and land cover-change (LULCC): Current status, challenges and prospects," *Sci. Total Environ.*, vol. 822, pp. 153559–153559, 2022.

[16] X. Wu, X. Liu, D. Zhang, J. Zhang, J. He, and X. Xu, "Simulating mixed land-use change under multi-label concept by integrating a convolutional neural network and cellular automata: A case study of Huizhou, China," *GIScience Remote Sens.*, vol. 59, pp. 609–632, 2022.

[17] S. Yousefi et al., "Image classification and land cover mapping using Sentinel-2 imagery: Optimization of SVM parameters," *Land*, vol. 11, no. 7, 2022, Art. no. 993.

[18] X. Pan, Z. Wang, Y. Gao, X. Dang, and Y. Han, "Detailed and automated classification of land use/land cover using machine learning algorithms in Google Earth Engine," *Geocarto Int.*, vol. 37, pp. 5415–5432, 2022.

[19] O. Akar and E. T. Gormus, "Land use/land cover mapping from airborne hyperspectral images with machine learning algorithms and contextual information," *Geocarto Int.*, vol. 37, pp. 3963–3990, 2022.

[20] X. Guo, J. Ye, and Y. Hu, "Analysis of land use change and driving mechanisms in Vietnam during the period 2000–2020," *Remote Sens.*, vol. 14, 2022, Art. no. 1600.

[21] U. Ali, T. J. Esau, A. A. Farooque, Q. U. Zaman, F. Abbas, and M. F. Bilodeau, "Limiting the collection of ground truth data for land use and land cover maps with machine learning algorithms," *ISPRS Int. J. Geo-Inf.*, vol. 11, 2022, Art. no. 333.

[22] K. S. S. Parthasarathy and D. P. Chandra, "Spatio-temporal classification and prediction of land use and land cover change for the Vembanad Lake system, Kerala: A machine learning approach," *Environ Sci. Pollut. Res. Int.*, vol. 29, pp. 86220–86236, 2022.

[23] W. Yanqiang et al., "The United Nations sustainable development goals (SDG) and the response strategies of China," *Adv. Earth Sci.*, vol. 33, pp. 1084–1093, 2018.

[24] J. E. Krauss, "Unpacking SDG 15, its targets and indicators: Tracing ideas of conservation," *Globalizations*, vol. 19, pp. 1179–1194, 2022.

[25] Z. Zhang, B. Hu, and H. Qiu, "Comprehensive evaluation of resource and environmental carrying capacity based on SDGs perspective and three-dimensional balance model," *Ecol. Indicators*, vol. 138, 2022, Art. no. 108788.

[26] M. Dallimer and L. C. Stringer, "Informing investments in land degradation neutrality efforts: A triage approach to decision making," *Environ. Sci. policy*, vol. 89, pp. 198–205, 2018.

[27] R. Sawut, Y. Li, A. Kasimu, and X. Ablat, "Examining the spatially varying effects of climatic and environmental pollution factors on the NDVI based on their spatially heterogeneous relationships in Bohai Rim, China," *J. Hydrol.*, vol. 617, 2023, Art. no. 128815.

[28] S. Tang, L. Song, S. Wan, Y. Wang, Y. Jiang, and J. Liao, "Long-time-series evolution and ecological effects of coastline length in Coastal Zone: A case study of the Circum-Bohai Coastal Zone, China," *Land*, vol. 11, 2022, Art. no. 1291.

[29] Y. Liu, X. Hou, X. Li, B. Song, and C. Wang, "Assessing and predicting changes in ecosystem service values based on land use/cover change in the Bohai Rim coastal zone," *Ecol. Indicators*, vol. 111, 2019, Art. no. 106004.

[30] Q. U. Yanbo, W. Xia, W. Shilei, Z. Weiya, P. Zongli, and W. Sen, "Spatio-temporal evolution and coupling characteristics of urban scale expansion and quality growth in Bohai Rim," *Geographical Res.*, vol. 40, pp. 762–778, 2021.

[31] G. Liying, W. Daolong, and Q. Jianjun, "Regional landscape pattern changes surrounding the Bohai Bay in China," *Resour. Sci.*, vol. 31, pp. 2144–2149, 2009.

[32] M. Gai, D. Liu, and Q. Benliang, "The research for spatial-temporal differentiation and influence factors of green marine economic efficiency in China," *Ecol. Econ.*, vol. 32, pp. 97–103, 2016.

[33] M. Jia, Z. Wang, D. Mao, C. Ren, C. Wang, and Y. Wang, "Rapid, robust, and automated mapping of tidal flats in China using time series Sentinel-2 images and Google Earth Engine," *Remote Sens. Environ.*, vol. 255, 2021, Art. no. 112285.

[34] M. Huijuan, G. Xiaohong, and G. Xiaotian, "Random forest classification of Landsat 8 imagery for the Complex terrain area based on the combination of spectral, topographic and texture information," *J. Geo-Inf. Sci.*, vol. 21, pp. 359–371, 2019.

[35] X. Li, C. Sun, H. Meng, X. Ma, G. Huang, and X. Xu, "A novel efficient method for land cover classification in fragmented agricultural landscapes using Sentinel satellite imagery," *Remote Sens.*, vol. 14, 2022, Art. no. 2045.

[36] Y. Zhao et al., "Classification of Zambian grasslands using random forest feature importance selection during the optimal phenological period," *Ecol. Indicators*, vol. 135, 2022, Art. no. 108529.

[37] A. Naboureh, H. Ebrahimy, M. Azadbakht, and M. Amani, "RUESVMs: An ensemble method to handle the class imbalance problem in land cover mapping using Google Earth Engine," *Remote Sens.*, vol. 12, no. 21, 2020, Art. no. 3484.

[38] P. Olofsson, G. M. Foody, M. Herold, S. V. Stehman, C. E. Woodcock, and M. A. Wulder, "Good practices for estimating area and assessing accuracy of land change," *Remote Sens. Environ.*, vol. 148, pp. 42–57, 2014.

[39] J. Wang, J. Zhang, N. Xiong, B. Liang, Z. Wang, and E. L. Cressey, "Spatial and temporal variation, simulation and prediction of land use in ecological conservation area of Western Beijing," *Remote Sens.*, vol. 14, no. 6, 2022, Art. no. 1452.

[40] W. U. Wenting, T. Bo, Z. Yunxuan, S. Minyan, Q. I. Xianyun, and X. U. Wei, "The trends of coastal reclamation in China in the past three decades," *Acta Ecologica Sinica*, vol. 36, pp. 5007–5016, 2016.

[41] X. X. Gu, X. Gao, H. Ma, F. Shi, X. Liu, and X. Cao, "Comparison of machine learning methods for land use/land cover classification in the complicated terrain regions," *Remote Sens. Technol. Appl.*, vol. 34, pp. 57–67, 2019.

[42] S. A. Adelabu and K. A. Adepoju, "Improving accuracy evaluation of Landsat-8 OLI using image composite and multisource data with Google Earth Engine," *Remote Sens. Lett.*, vol. 11, pp. 107–116, 2020.

[43] A. E. Maxwell, T. A. Warner, and F. Fang, "Implementation of machine learning classification in remote sensing: An applied review," *Int. J. Remote Sens.*, vol. 39, no. 9, pp. 2784–2817, 2018.

[44] Y. O. Ouma, A. Keitsile, B. Nkwae, P. Odirile, D. Moalafhi, and J. Qi, "Urban land-use classification using machine learning classifiers: Comparative evaluation and post-classification multi-feature fusion approach," *Eur. J. Remote Sens.*, vol. 56, no. 1, 2023, Art. no. 2173659.

[45] M. A. Chandra and S. S. Bedi, "Survey on SVM and their application in image classification," *Int. J. Inf. Technol.*, vol. 13, pp. 1–11, 2021.

[46] D. Ya-kun, W. Yu, H. Zi-ling, W. Peng, Z. Hao, and Z. Wei-jun, "Comparison of land use/cover classification algorithms in the Erhai Watershed based on GEE," *J. Northwest Forestry Univ.*, vol. 39, pp. 28–35, 2024.
[47] Z. Binghua, Z. Yili, G. Changjun, and W. Bo, "Land cover classification based on random forest and feature optimism in the Southeast Qinghai-Tibet Plateau," *Scientia Geographica Sinica*, vol. 43, pp. 388–397, 2023.
[48] N. Gorelick, M. Hancher, M. Dixon, S. Ilyushchenko, D. Thau, and R. Moore, "Google Earth Engine: Planetary-scale geospatial analysis for everyone," *Remote Sens. Environ.*, vol. 202, pp. 18–27, 2017.
[49] W. Ruiqing, Z. Mingxiang, W. Haitao, and L. Yuanhui, "Analysis on wetland definition and classification of the wetland conservation law of the People's Republic of China," *Wetland Sci.*, vol. 20, pp. 404–412, 2022.
[50] S. Jin et al., "Spatial-temporal changes of land use/cover change and habitat quality in Sanjiang plain from 1985 to 2017," *Front. Environ. Sci.*, vol. 10, pp. 86220–86236, 2022.
[51] C. Zhang, H. Tan, M. Zhou, and Z. Wang, "What was the China's spatial-temporal evolution characteristics of cross-sensitivity of ecosystem service value under land use transition? A case study of the Jiangjin, Chongqing," *Front. Environ. Sci.*, vol. 10, 2022, Art. no. 1080809.

Lina Ke received the B.S. degree in surveying and mapping from Jilin University, Changchun, China, in 1997, the M.Agr. degree in cartography and geographic information systems from the Chengdu University of Technology, Chengdu, China, in 2001, and the Ph.D. degree in hydrology and water resources from the Dalian University of Technology, Dalian, China, in 2013.

She is currently a Professor and Doctoral Supervisor with Liaoning Normal University, Dalian, China. She is also the Director of the Liaoning Provincial Geographical Society and Liaoning Provincial Oceanographic Society. She has been the PI for more than 30 national and provincial sponsored projects. She has authored or coauthored more than 80 scientific papers in the areas of her interest. Her research interests include remote sensing applications for ecosystem and land-surface dynamics, geointelligent computing, and coastal environment monitoring.

Daqi Liu received the master's degree in physical geography in 2020 from Liaoning Normal University, Dalian, China, where he is currently working toward the doctoral degree in cartography and geographic information systems with the College of Geographical Sciences.

His research interests include coastal remote sensing and wetland remote sensing.

Qin Tan received the bachelor's degree in geographic information science from Tianjin Normal University, Tianjin, China, in 2020. She is currently working toward the postgraduate degree with Liaoning Normal University, Dalian, China, majoring in cartography and geographic information systems.

Her study area is coastal wetland remote sensing.

Shuting Wang received the master's degree in cartography and geographic information systems from the School of Geographic Sciences, Liaoning Normal University, Dalian, China, in 2022.

She is currently working with the Liaoning Seismological Bureau. Her main research interest focuses on wetland remote sensing.

Quanming Wang received the B.S. degree in surveying and mapping from Jilin University, Changchun, China, in 1996, the M.Agr. degree in environmental science from the Dalian Maritime University, Dalian, China, in 2008, and the Ph.D. degree in environmental science from the Ocean University of China, Qingdao, China, in 2016.

He is currently a Senior Engineer and a master tutor. He is also the Deputy Director of the National Key Laboratory of Environmental Protection, Marine Ecological Environment Improvement and Restoration, and the Director of China Marine Development Research Association, Thousand-Level Talent of Liaoning Province's Talent Plan. His research interests include marine resources and environment management, marine space planning, and marine ecological environment management and restoration.

Jun Yang received the Ph.D. degree in human geography from the College of Urban and Environmental Sciences, Liaoning Normal University, Dalian, China, in 2009.

He is a Professor and Doctoral Supervisor and a 2023 Clarivate Global Highly Cited Scholar (candidate), 2022 Elsevier China Highly Cited Scholar, 2023 Stanford University in the United States Highly Cited Scholar, 2023 Global Top 2% Scientists, Science and Technology Leader of Xingliao Talent Program, Liaoning Province, Hundreds of Millions of Talents, and the Director of China Association of Land Economics. He is the Deputy Director of the Liaoning Provincial Key Laboratory of Environmental Computing and Sustainable Development, a member of the Urban Geography Professional Committee of the Chinese Geographical Society, the Standing Director of the Liaoning Provincial Geographical Society, and an expert of the Planning Committee of the Dalian Municipal Natural Resources Bureau. His main research interests include land use change simulation, urban climate, and human settlement management.